

Synthesis, Characterization, Toxicity Analysis and *in silico* Evaluation of New 1,4-Benzopyrone Analogue against Human Metapneumovirus (HMPV) and Respiratory Syncytial Virus (RSV)

MOHAMMAD AUWAL SA'AD^{1,2}, MANICKAM RAVICHANDRAN^{1,2}, SHIVKANYA FULORIA^{3,*},
VETRISELVAN SUBRAMANIYAN⁴, PANKAJ AGRAWAL⁵, GAUTAM BHARDWAJ⁵ and NEERAJ KUMAR FULORIA^{3,*}

¹Department of Biotechnology, Faculty of Applied Science, AIMST University, Bedong 08100, Kedah, Malaysia

²Centre of Excellence for Vaccine Development (CoEVD), Faculty of Applied Science, AIMST University, Bedong 08100, Kedah, Malaysia

³Faculty of Pharmacy, AIMST University, Bedong Kedah, Malaysia

⁴Department of Medical Sciences, School of Medical and Life Sciences, Sunway University No. 5, Jalan Universiti, Bandar Sunway, 47500 Selangor Darul Ehsan, Malaysia

⁵Guru Gobind Singh Indraprastha University, Government of NCT of Delhi, Sector 16C, Dwarka, New Delhi-110078, India

*Corresponding authors: E-mail: shivkanya_fuloria@aimst.edu.my; nfuloria@aimst.edu.my

Received: 11 November 2024;

Accepted: 25 January 2025;

Published online: 31 January 2025;

AJC-21901

The global threat posed by recent respiratory viruses necessitates the development of novel antiviral agents. This study focused on the design, synthesis, characterization and cytotoxicity evaluation of two new coumarin analogues, 4-((5-(4-hydroxyphenyl)-1,3,4-oxadiazol-2-yl)methoxy)-2H-benzopyrone (**4**) and N-(4-chloro-benzylidene)-2-((2H-benzopyrone-4-yl)oxy)acetohydrazide (**5**). These compounds were synthesized from hydrazide derivative of benzopyrone (**3**) through reactions with 4-hydroxybenzoic acid and 4-chlorobenzaldehyde, respectively. Structural confirmation was achieved using IR, NMR and mass spectrometry. The cytotoxicity was assessed using the MTT assay, demonstrating significant cell viability in HEK-293 cells. Molecular docking studies were performed to evaluate the interaction of the synthesized compounds with RNA-dependent RNA polymerases of human metapneumovirus (HMPV) (PDB ID: 8FPJ) and respiratory syncytial virus (RSV) (PDB ID: 8FPI). Both compounds exhibited high docking scores, indicating strong potential for inhibiting these essential viral enzymes. These findings highlight compounds **4** and **5** as promising candidates for further development as antiviral agents targeting HMPV and RSV. Interestingly, this is the first-time investigation in which benzopyrones have been explored to exhibit significant *in silico* activity against HMPV. However, future studies should be focused on their preclinical evaluation to establish their therapeutic potential in HMPV treatment.

Keywords: Coumarin, Synthesis, Molecular docking, Respiratory syncytial virus, Human metapneumovirus.

INTRODUCTION

In recent decades, benzopyrone derivatives have attracted high attention of investigators attributed of their various therapeutic properties including antiviral potential [1,2]. Benzopyrone is a heterocyclic compound that comprises a substituted keto group on a pyran ring, which is mainly responsible for offering diverse biological properties including antiviral activity [3]. The recent pandemic and the emergence of new respiratory viruses have drawn significant attention from researchers to investigate benzopyrones as potential antiviral agents. Several studies have demonstrated the antiviral properties of benzopyrones and their derivatives. Notably, evidence suggests that

hesperetin, a benzopyrone derivative, can inhibit SARS-CoV-2 by interfering with viral replication [4]. Reports suggest that benzopyrones could also inhibit the replication of respiratory syncytial virus (RSV) and overcome the mucus barriers of human bronchial epithelial (HBE) cell cultures [5].

A molecular docking study revealed benzopyrones to inhibit coronavirus by inhibiting 3CL^{pro} a chymotrypsin-like protease. Surprisingly, the inhibitory potential of benzopyrones was found to be better than lopinavir the commercially available antiviral drugs [6]. Another study highlighted benzopyrene antiviral potential against nucleocapsid and NTD of SARS-CoV-1, SARS-CoV-2, MERS-CoV, HCoV-OC43, HCoV-NL63, HCoV-229E and HCoV-HKU1, as offered good binding

and very less cytotoxicity against MRC-5 and A549 cell lines [7]. The recent outbreak of human metapneumovirus (HMPV) alerted the investigators, but facts suggest that currently, no specific treatment is available for HMPV [8]. Hence, based on the evidence of the antiviral properties of benzopyrones [9], the present study was intended to perform the synthesis, characterization, toxicity analysis and molecular docking analysis of some benzopyrones against HMPV RNA-dependent RNA polymerase with MRK-1 (PDB id: 8FPJ) and respiratory syncytial virus (RSV) RNA-dependent RNA polymerase with MRK-1 (PDB id: 8FPI). Importantly, this is the first time *in silico* experimental study where in benzopyrones are reported to exhibit high activity against HMPV.

EXPERIMENTAL

Chemicals and reagents for the synthesis of benzopyrones were procured from Merck KGaA, Sigma-Aldrich, HmbG® Chemicals, Friendemann Schmidt and Qrec Chemicals. The characterization was performed using ASCEND™ NMR spectrometer, ATR-FTIR and Direct Infusion IonTrapMass spectrometer. The purity of compounds was determined by the SMP11 Analogue apparatus. The progress of reaction was determined by TLC using CHCl₃:CH₃OH as a solvent system.

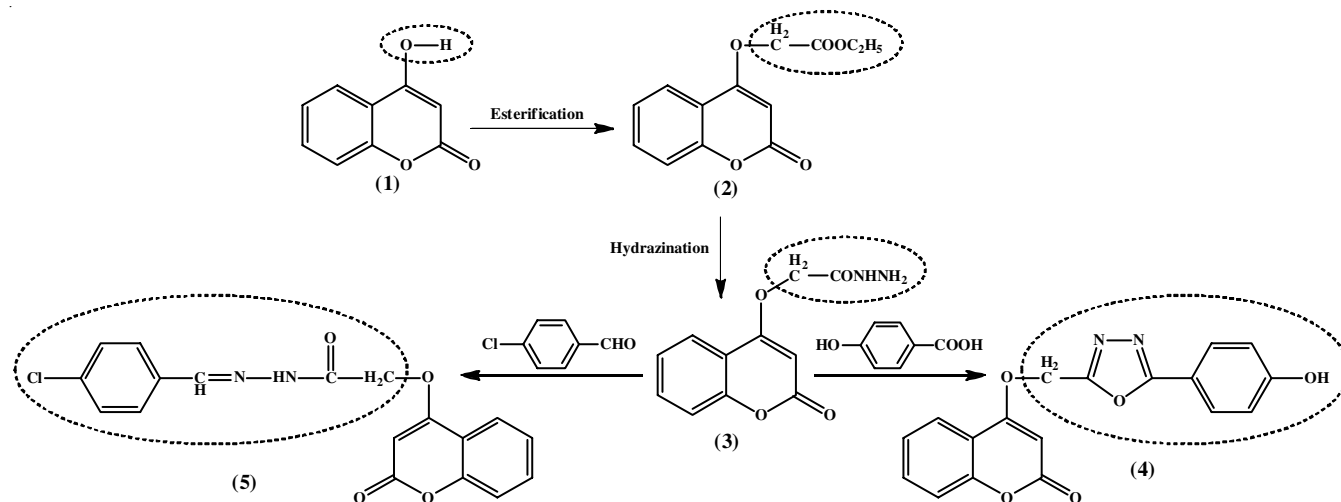
Synthesis of 4-((5-(4-hydroxyphenyl)-1,3,4-oxadiazolyl)-methoxyl)-2H-benzopyrone (4): Synthesis of compound 4 was performed as per the standard reference with minor modifications [10,11]. Briefly, compound 3 (0.001 mol) previously synthesized by hydrazination of ester derivative (2) of 4-hydroxybenzopyran-2-one (1) was added to 20 mL phosphoryl chloride. To this mixture, an equimolar concentration of 4-hydroxybenzoic acid (0.001 mol) was added. The solution was mixed gently and refluxed for 8 h in an anhydrous condition. The resulting precipitate was cooled, washed with ice, filtered with Whatman paper and recrystallized with activated charcoal and methanol to obtain pure compound 4 (Scheme-I). The TLC for synthesized oxadiazole was done by dissolving their crystals into 1 mL methanol with a solvent ratio of chloroform:methanol (1.7:0.3) to determine its purity. IR (KBr, ν_{\max} , cm⁻¹): 1588.2 (C=N str.), 1672.6 (C=O str.), 2922.9 (C-H str.) and 3190.4 (N-H str.); ¹H NMR (DMSO, ppm) δ : 9.8 (s, NH), 8.5 (s,

N=CH), 6.8-7.9 (m, Ar-H), 5.5 (s, =CH) and 4.6 (s, OCH₂); ¹³C NMR (DMSO, δ ppm): 61 (O-CH₂), 91 (=CH), 141 (N=C), 113-155 (Ar-C), 163 (C=O), 170 (C=C in pyran), 193 (N-C=O); Mass (*m/z*): 356.

N-(4-Chloro-benzylidene)-2-((2H-benzopyrone)oxy)-acetohydrazide (5): Synthesis of compound 4 was performed as per the standard reference with minor modifications [12]. Initially, compound 3 (0.002 mol) and an equimolar concentration of 4-chloro benzaldehyde were dissolved into a sufficient quantity of absolute ethanol. To this mixture, 0.1 mL of glacial acetic acid was added and then refluxed the reaction mixture for 6 h. After the completion of reaction, the excess solvent was removed under reduced pressure. The precipitate formed after cooling was filtered using Whatman filter paper. The resultant mixture (Schiff base) was dried and recrystallized to offer pure compound 5. The TLC for Schiff base was done by dissolving their crystals into 1 mL methanol with a ratio of solvent (CHCl₃:CH₃OH (1.7:0.3) to determine the purity of compound 5. IR (KBr, ν_{\max} , cm⁻¹): 3190.4 (N-H str.), 2919.4 (C-H str.), 1731.2 (C=O str.), 1601.6 (C=N str.), 1201.2 (C-O-C str. oxadiazole ring); ¹H NMR (DMSO, δ ppm): 9.8 (s, NH), 8.5 (s, N=CH), 6.6-7.7 (m, Ar-H), 5.7 (s, =CH), 3.1 (s, OCH₂); ¹³C NMR (DMSO, δ ppm): 65 (O-CH₂), 91 (=CH), 111-155, (Ar-C), 160, (C=N), 168 (C=O), 170 (C=C in pyran); Mass (*m/z*): 336.

Cell viability: The synthesized compounds 4 and 5 were further subjected to cell viability study using MTT assay as per ATCC guidelines and previous standard protocol protocols [13]. HEK-293 cells were cultured in a 96-well plate, incubated overnight, treated with test compounds 4 and 5 (1000-7.8 μ g/mL) and incubated for 24 h. Subsequently, the MTT reagent was introduced to the cells in the plate, followed by incubation to facilitate the formation of formazan crystals, which were then solubilized with DMSO and analyzed for absorbance at 570 nm, using a reference wavelength of 650 nm. The data was analyzed to determine % cell viability by comparing it with control. This experiment was done in triplicate and % cell viability was determined using the following expression (eqn. 1):

$$\text{Cell viability (\%)} = \frac{\text{Sample absorbance (Treated cells)}}{\text{Control absorbance}} \times 100 \quad (1)$$



Scheme-I: Synthesis of benzopyrones (4 & 5)

TABLE-1
CELL VIABILITY STUDY DATA FOR COMPOUNDS 1-5 AGAINST HEK-293 CELLS

Compd.	Concentration (μg)							
	1 mg	500	250	125	62.5	31.25	15.625	7.8125
1	47.05 \pm 0.01*	54.18 \pm 0.02*	54.95 \pm 0.01*	59.45 \pm 0.02*	64.95 \pm 0.01 ^{ns}	72.37 \pm 0.00 ^{ns}	77.02 \pm 0.01 ^{ns}	85.17 \pm 0.05 ^{ns}
2	37.59 \pm 0.07*	39.23 \pm 0.05*	42.34 \pm 0.06*	51.48 \pm 0.04*	54.99 \pm 0.07*	68.38 \pm 0.02 ^{ns}	77.99 \pm 0.03 ^{ns}	84.67 \pm 0.06 ^{ns}
3	65.44 \pm 0.00*	68.14 \pm 0.02*	73.55 \pm 0.01 ^{ns}	88.58 \pm 0.00 ^{ns}	91.27 \pm 0.02 ^{ns}	93.57 \pm 0.02 ^{ns}	95.52 \pm 0.00 ^{ns}	97.43 \pm 0.00 ^{ns}
4	54.29 \pm 0.00*	54.76 \pm 0.00*	56.9 \pm 0.00*	60.34 \pm 0.01*	68.12 \pm 0.00 ^{ns}	70.9 \pm 0.03 ^{ns}	82.37 \pm 0.01 ^{ns}	88.05 \pm 0.03 ^{ns}
5	69.64 \pm 0.00*	70.45 \pm 0.00 ^{ns}	72.79 \pm 0.02 ^{ns}	79.39 \pm 0.02 ^{ns}	95.27 \pm 0.02 ^{ns}	95.51 \pm 0.00 ^{ns}	96.77 \pm 0.00 ^{ns}	96.86 \pm 0.00 ^{ns}
Control	91.39	92.45	92.66	93.01	94.91	96.15	97.77	100

Data are expressed as mean \pm standard deviation of the mean with each experiment performed in triplicate. Statistical significance is indicated by * $p < 0.05$ and ns no statistically significant difference when compared to control (untreated cells).

Molecular docking: The *in silico* molecular docking study involved docking of synthesized benzopyrones to assess their interaction with the target HMPV RNA-dependent RNA polymerase with MRK-1 (8FPJ) and RSV RNA-dependent RNA polymerase with MRK-1 (8FPI) using Intel i7 and 16 GB RAM. Protein preparation involved Discovery Studio, ChemDraw and Open Babel for structure drawing and conversion to working format software [14,15]. All designed chemical structures were modelled using Chemskech software. The compound's 2D structures were generated and converted into 3D structures by Ligplot. Designed structures were subjected to optimization energy minimization (by AutoDock) and molecular docking [16]. The HMPV (8FPJ) and RSV (8FPI) 3D structures were downloaded from the RCSB Protein Data Bank. Downloaded HMPV and RSV proteins were prepared using Discovery Studio Visualizer by removal of water molecules and heteroatoms. For hydrogen addition and charges assignment molecular graphics laboratory (MGL) tools were used. To define grid parameters and docking AutoDock Vina was used and finally, the results of docking were analyzed using Discovery Studio Visualizer [17].

RESULTS AND DISCUSSION

The challenges posed by the recent pandemic, the outbreak of new respiratory viruses [18] and the cytotoxicity concerns associated with new chemical entities, combined with the high antiviral potential of benzopyrones, served as the motivation for this study. This research focused on the synthesis, characterization, toxicity analysis and molecular docking evaluation of select benzopyrones against the RNA-dependent RNA polymerase of HMPV (PDB ID: 8FPJ) and RSV (PDB ID: 8FPI), both bound to MRK-1. Based on the evidence [12,19], this study involved the design of **Scheme-I**, which successfully yielded compounds in significant amounts. The treatment of a hydrazide derivative of benzopyrone (**3**) with 4-hydroxybenzoic acid resulted in an oxadiazole derivative of benzopyrone (**4**) via a cyclization reaction. Meanwhile, the treatment of compound **3** with 4-chlorobenzaldehyde produced an imino derivative of benzopyrone (**5**) through a Schiff's base reaction. The synthesis was carried out under anhydrous conditions and the purification of the synthesized compounds was achieved through recrystallization using methanol. Purity was confirmed by assessing the melting points and observing single-spot patterns in TLC analysis [20]. The structures of the synthesized compounds were characterized using IR, NMR and mass spectral

data, which aligned with the assigned structures of compounds **4** and **5**. Additionally, the characterization data were cross-referenced with existing literature [10-12], further validating the findings.

Cell viability studies: The cell viability (toxicity) analysis of the synthesized compounds was evaluated using the MTT assay in a 96-well plate format against HEK-293 cells [21]. The percentage of cell viability was calculated using the formula provided in eqn. 1 and the experiment was conducted following standard protocols [22]. The results demonstrated that all the synthesized compounds exhibited significant safety compared to the control group, as no toxicity was observed in HEK-293 cells. This confirms the safety profile of the synthesized compounds. Detailed cell viability results are presented in Tables 1 and 2, which were further validated against data from previous studies [21,22]. Among the tested compounds, **4** and **5** showed the highest safety margins, with CC_{50} data indicating their minimal toxicity to HEK-293 cells. These findings position compounds **4** and **5** as the least toxic and most biocompatible candidates, supporting their further development for antiviral applications.

TABLE-2
 CC_{50} OF COMPOUNDS 1-5 AGAINST HEK-293 CELLS

Compounds	CC_{50} ($\mu\text{g/mL}$)
1	87.89
2	92.6
3	254.8
4	500.55
5	4596

Molecular docking studies: The *in silico* docking experiment was conducted to evaluate the binding affinity of the synthesized compounds to the active site of HMPV RNA-dependent RNA polymerase (PDB ID: 8FPJ) and RSV RNA-dependent RNA polymerase (PDB ID: 8FPI) complexed with MRK-1 [18]. The docking scores, which indicate the strength of the interaction between the compounds and the target proteins, are shown in Table-3. These results provide critical insights into the potential of the synthesized compounds as inhibitors of RNA-dependent RNA polymerase, supporting their candidacy for further antiviral development.

All the synthesized compounds were found to occupy the active sites of HMPV RNA-dependent RNA polymerase (PDB ID: 8FPJ) complexed with MRK-1. Among them, compounds **4** and **5** exhibited the highest docking scores (D-scores), sug-

TABLE-3
DOCKING SCORE OF SYNTHESIZED
COMPOUNDS AGAINST 8FPJ AND 8FPI

Compounds	Docking score	
	8FPJ	8FPI
1	-6.4	-7.0
2	-6.0	-7.1
3	-7.9	-7.5
4	-8.1	-7.6
5	-8.1	-7.9
Ligand	-8.0	-7.9

esting their strong potential activity against both HMPV and RSV. These results highlight the high inhibitory potential of compounds **4** and **5** against the target viruses. The 2D ligand interaction images of compounds **4** and **5** with 8FPJ are shown in Figs. 1 and 2, respectively. These diagrams depict significant interactions with specific amino acid residues in the active

site of 8FPJ, further validating their binding efficiency and potential as antiviral agents.

The 2D ligand interaction diagram for compound **4** (Fig. 1) confirms the formation of key hydrogen bonds that contribute to its binding affinity with the active site of HMPV RNA-dependent RNA polymerase (PDB ID: 8FPJ) complexed with MRK-1. A hydrogen bond was observed between the oxygen atom of the pyrone ring and arginine (Arg-572) in the chain; another hydrogen bond was formed between the hydroxy group's hydrogen atom and lysine (Lys-554) in the chain. These interactions play a crucial role in stabilizing the ligand-protein complex, enhancing the binding affinity of compound **4**. The 3D arrangement of the molecular docking complex strengthens these interactions, demonstrating the manner in which compound **4** effectively occupies the active site of HMPV RNA-dependent RNA polymerase alongside MRK-1, as depicted in Fig. 1. These findings underscore the potential of compound **4** as an effective antiviral agent.

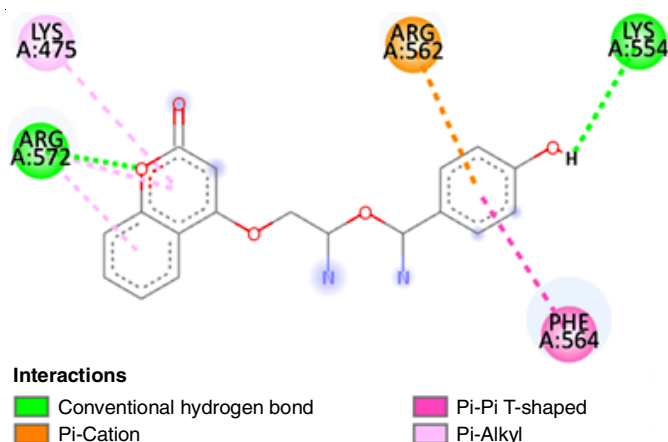


Fig. 1. 2D ligand interaction diagram and 3D docked pose of compound **4** with 8FPJ

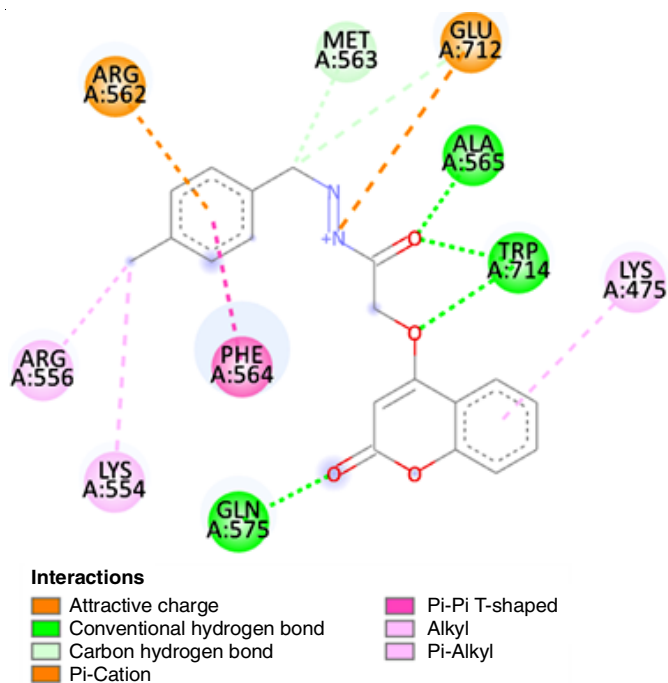
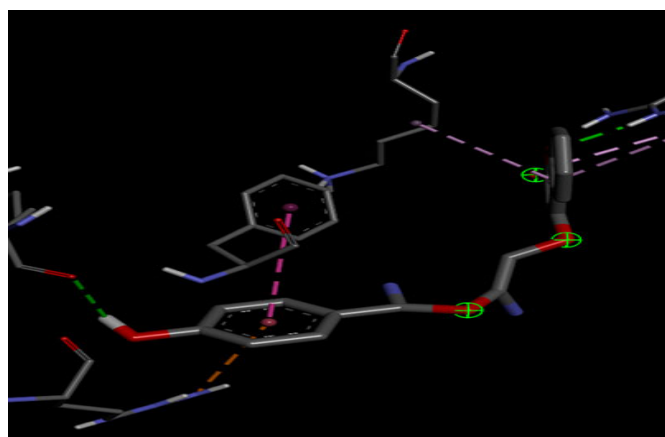


Fig. 2. 2D ligand interaction diagram and 3D docked pose of compound **5** with 8FPJ



The 2D ligand interaction diagram for compound **5** (Fig. 2) reveals several key hydrogen bonds that contribute to its binding affinity with the active site of HMPV RNA-dependent RNA polymerase (PDB ID: 8FPJ) complexed with MRK-1. A hydrogen bond was formed between the oxo group of pyrone ring and glycine (Gly-575) in the chain and the oxo group in the aliphatic chain formed hydrogen bonds with alanine (Ala-564) and tryptophan (Trp-714) in the chain. The oxygen atom of the aliphatic chain also interacted with tryptophan (Trp-714) in the chain. These interactions are critical for stabilizing the ligand-protein complex and enhancing the binding affinity of compound **5**. The 3D arrangement of the molecular docking complex strengthens these interactions, demonstrating the placement of compound **5** within the active site of HMPV RNA-dependent RNA polymerase alongside MRK-1, as depicted in Fig. 2. These findings also demonstrate the promising antiviral potential of compound **5**.

The 2D ligand interaction diagram for compound **4** (Fig. 3) reveals several crucial hydrogen bonds contributing to its binding affinity with the active site of RSV RNA-dependent RNA polymerase (PDB ID: 8FPI) complexed with MRK-1. A hydrogen bond was formed between the oxo group of the pyrone ring and tyrosine (Tyr-575) and arginine (Arg-995) in the chain. The hydroxy group formed hydrogen bonds with glycine (Gly-1069) and aspartic acid (Asp-1060) in the chain. The nitrogen atom of the oxadiazole ring inter-acted with methionine (Met-983) and leucine (Leu-984) residues in the chain. These interactions are essential for stabilizing the ligand-protein complex, enhancing the binding affinity of compound **4**. The 3D pose of the molecular docking complex further confirms these interactions, showing that compound **4** fits into the active site of RSV RNA-dependent RNA polymerase with MRK-1, as shown in Fig. 3. These findings indicate the promising, antiviral potential of compound **4** against RSV.

The 2D ligand interaction diagram for compound **5** (Fig. 4) reveals the formation of key hydrogen bonds contributing to its binding affinity with the active site of RSV RNA-dependent RNA polymerase (PDB ID: 8FPI) complexed with MRK-1.

Specifically, a hydrogen bond was formed between the nitrogen atom of the amido group and the proline (Pro-990) and arginine (Arg-995) residues in the chain. The 3D images of the molecular docking complex reinforces these interactions, demonstrating the manner compound **5** integrates into the active site of RSV RNA-dependent RNA polymerase alongside MRK-1, as shown in Fig. 4. Based on the *in silico* analysis, which demonstrates high docking scores for compounds **4** and **5**, along with their 2D ligand interaction diagrams and 3D docked poses, it is confirmed that compounds **4** and **5** exhibit strong inhibition properties against HMPV RNA-dependent RNA polymerase with MRK-1 (PDB ID: 8FPJ) and RSV RNA-dependent RNA polymerase with MRK-1 (PDB ID: 8FPI) as potential antiviral agents.

This study is the first to demonstrate that benzopyrone compounds (**4** and **5**) exhibit considerable interaction with HMPV and RSV, hence providing *in silico* evidence of their high potential against HMPV. So, this study recommends both benzopyrones (**4** and **5**) to be developed as anti-HMPV and anti-RSV agents through preclinical and clinical experimental studies.

Conclusion

The present study successfully synthesized and characterized a two benzopyrone derivatives (**4** and **5**), which demonstrate promising safety profiles against HEK-293 cells based on their CC_{50} values, supporting their potential for therapeutic application. Toxicity analysis confirmed that these compounds exhibit minimal cytotoxicity, further validating their suitability for drug development. The *in silico* molecular docking studies revealed significant binding affinities of compounds **4** and **5** against human metapneumovirus (HMPV) and respiratory syncytial virus (RSV) RNA-dependent RNA polymerases (PDB IDs: 8FPJ and 8FPI, respectively), with high docking scores and key interactions within the active sites of these enzymes. These findings suggest that compounds **4** and **5** possess antiviral potential against HMPV and RSV, making them promising candidates for future antiviral drug development. Significantly,

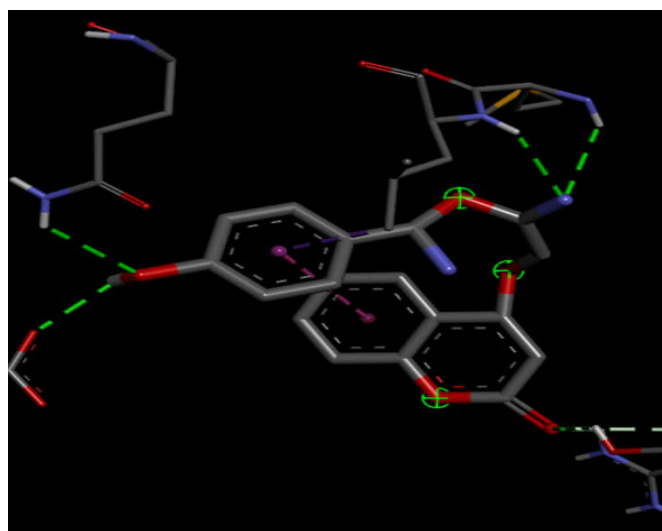
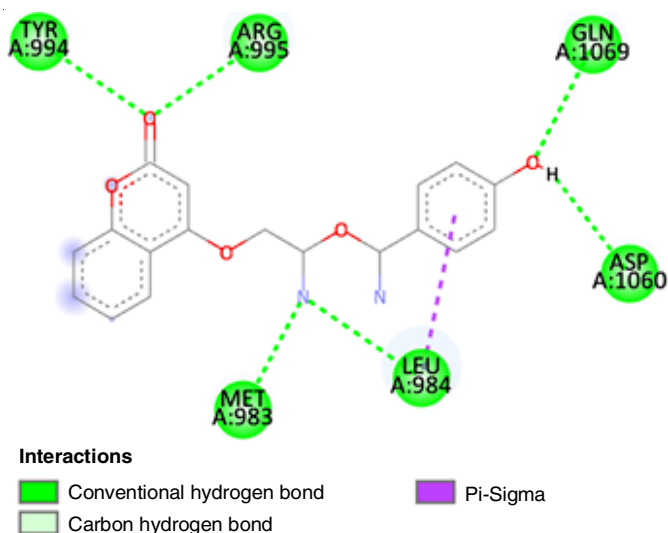


Fig. 3. 2D ligand interaction diagram and 3D docked pose of compound **4** with 8FPI

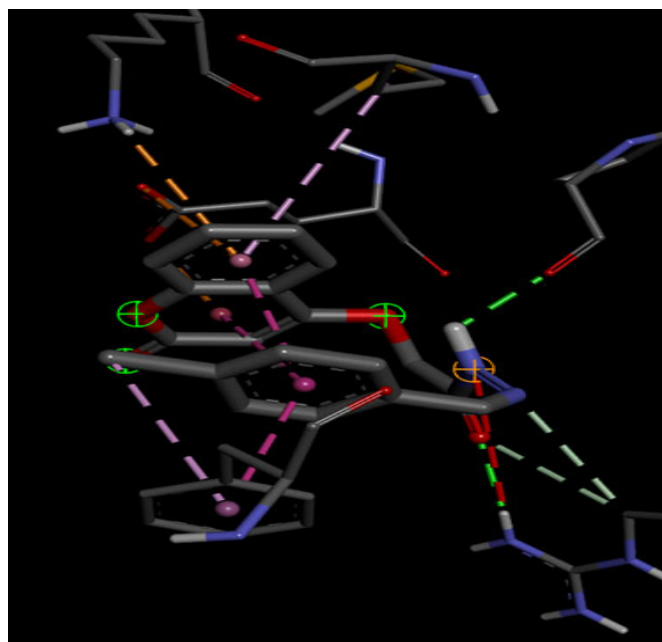
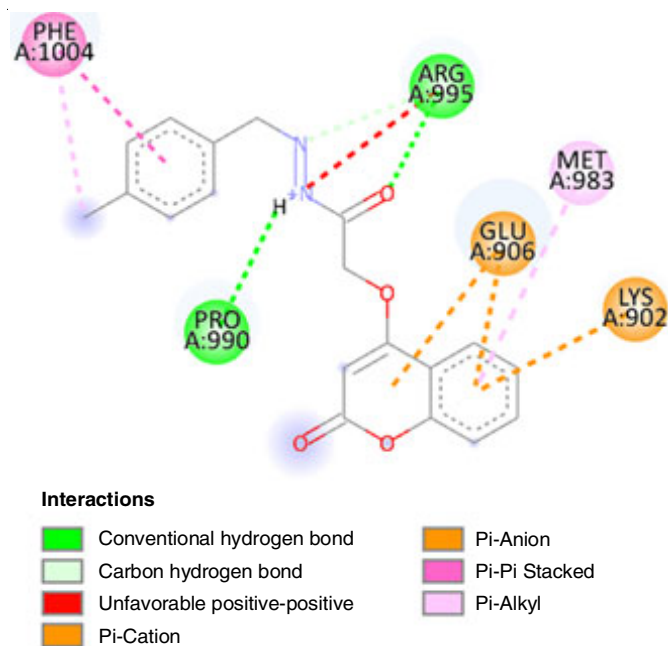


Fig. 4. 2D ligand interaction diagram and 3D docked pose of compound **5** with 8FPI

this is the first-time study wherein benzopyrones have been proven *in silico* to exhibit significant inhibition of HMPV. However, further preclinical validation and in-depth mechanistic studies are essential to confirm their efficacy and establish them as viable antiviral agents for clinical application.

ACKNOWLEDGEMENTS

This research was funded by the Ministry of Higher Education (MOHE) Malaysia, grant no. FRGS/1/2020/STG01/AIMST/01/1. The authors thank the Ministry of Higher Education (MOHE), Malaysia and AIMST University for financial support and assistance in completing this study.

CONFLICT OF INTEREST

The authors declare that there is no conflict of interests regarding the publication of this article.

REFERENCES

- R. Abdizadeh, F. Hadizadeh and T. Abdizadeh, *Mol. Divers.*, **26**, 1053 (2022); <https://doi.org/10.1007/s11030-021-10230-6>
- E. Gupta, E. Guliani and K. Bajaj, *Top. Curr. Chem.*, **382**, 16 (2024); <https://doi.org/10.1007/s41061-024-00462-z>
- W.R. Mendis, J.W. Lim, G.W. Kim and S.Y. Kang, *Aquaculture*, **585**, 740703 (2024); <https://doi.org/10.1016/j.aquaculture.2024.740703>
- P.K. Agrawa, C. Agrawal and G. Blunden, *Nat. Prod. Commun.*, **16**, 1 (2021); <https://doi.org/10.1177/1934578X211066723>
- J.M. de Sá, I. Thongpan, J.D. Busso, T.D. Rodrigues, P. Chen, A.L. Helena, L.O. Regasini, M.A. Fossey, Í.P. Caruso, F.P. de Souza and M.E. Peeples, *Int. J. Mol. Sci.*, **25**, 13301 (2024); <https://doi.org/10.3390/ijms252413301>
- M. Özdemir, B. Köksoy, D. Ceyhan, K. Sayin, E. Erçag, M. Bulut and B. Yalçin, *J. Biomol. Struct. Dyn.*, **40**, 4905 (2022); <https://doi.org/10.1080/07391102.2020.1863263>
- Y. Peng, N. Du, Y. Lei, S. Dorje, J. Qi, T. Luo, G.F. Gao and H. Song, *EMBO J.*, **39**, e105938 (2020); <https://doi.org/10.15252/emj.2020105938>
- Y. Feng, T. He, B. Zhang, H. Yuan and Y. Zhou, *Virolog. J.*, **21**, 59 (2024); <https://doi.org/10.1186/s12985-024-02327-9>
- S. Mishra, A. Pandey and S. Manvati, *Heliyon*, **6**, e03217 (2020); <https://doi.org/10.1016/j.heliyon.2020.e03217>
- R. Hamdy, S.A. Elseginy, N.I. Ziedan, M. El-Sadek, E. Lashin, A.T. Jones and A.D. Westwell, *Int. J. Mol. Sci.*, **21**, 8980 (2020); <https://doi.org/10.3390/ijms21238980>
- A. Kumar Madugula, B. Kiran, B.N. Suresh Varma Dendukuri, T.V.N. Kishore, P. Srinivasa Rao, G. Ranagaih and K. Jagadeesh, *Results Chem.*, **9**, 101664 (2024); <https://doi.org/10.1016/j.rechem.2024.101664>
- P.M. Thakor, J.D. Patel, R.J. Patel, S.H. Chaki, A.J. Khimani, Y.H. Vaidya, A.P. Chauhan, A.B. Dholakia, V.C. Patel, A.J. Patel, N.H. Bhavsar and H.V. Patel, *ACS Omega*, **9**, 35431 (2024); <https://doi.org/10.1021/acsomega.4c02007>
- N.S. El-Sayed, M.I. Sajid, K. Parang and R.K. Tiwari, *Int. J. Biol. Macromol.*, **191**, 1204 (2021); <https://doi.org/10.1016/j.ijbiomac.2021.09.160>
- Hunter AD. ACD/ChemSketch 1.0 (freeware); ACD/ChemSketch 2.0 and its tautomers, dictionary, and 3D plug-ins; ACD/HNMR 2.0; ACD/CNMR 2.0.
- A. Drefahl, *J. Cheminform.*, **3**, 1 (2011); <https://doi.org/10.1186/1758-2946-3-1>
- O. Trott and A.J. Olson, *J. Comput. Chem.*, **31**, 455 (2010); <https://doi.org/10.1002/jcc.21334>
- P. Bhardwaj, G.P. Biswas, N. Mahata, S. Ghanta and B. Bhunia, *Chemosphere*, **293**, 133550 (2022); <https://doi.org/10.1016/j.chemosphere.2022.133550>
- V.A. Kleiner, T. O. Fischmann, J.A. Howe, D.C. Beshore, M.J. Eddins, Y. Hou, T. Mayhood, D. Klein, D.D. Nahas, B.J. Lucas, E. Murray, H. Xi, D.Y. Ma, K. Getty and R. Fearn, *Commun. Biol.*, **6**, 649 (2023); <https://doi.org/10.1038/s42003-023-04990-0>
- S.J. Hamid and T. Salih, *Drug Des. Devel. Ther.*, **16**, 2275 (2022); <https://doi.org/10.2147/DDDT.S364746>
- A.A. Siddiqui, R. Mishra and M. Shaharyar, *Eur. J. Med. Chem.*, **45**, 2283 (2010); <https://doi.org/10.1016/j.ejmech.2010.02.003>
- M. Shaharyar, A. Mazumder, Salahuddin, R. Garg and R.D. Pandey, *Arab. J. Chem.*, **9**, S342 (2016); <https://doi.org/10.1016/j.arabjc.2011.04.013>
- G. Khodarahmi, E. Taherian, M. Khajouei, F. Hassanzadeh and N. Dana, *Res. Pharm. Sci.*, **14**, 247 (2019); <https://doi.org/10.4103/1735-5362.258493>